Weierstraß–Institut
für Angewandte Analysis und Stochastik

im Forschungsverbund Berlin e.V.

Preprint ISSN 0946 – 8633

Mathematical Modeling and Numerical Simulation of Semiconductor Detectors

H. Gajewski[1], H.–Chr. Kaiser[1], H. Langmach[1], R. Nürnberg[1], and

R. H. Richter[2]

submitted: 17 Jan 2001

[1] Weierstraß-Institut
für Angewandte Analysis und Stochastik
Mohrenstraße 39
D–10117 Berlin
Germany
E-Mail: gajewski@wias-berlin.de
E-Mail: kaiser@wias-berlin.de
E-Mail: langmach@wias-berlin.de
E-Mail: nuernberg@wias-berlin.de

[2] MPI Halbleiterlabor
Otto Hahn Ring 6
D–81739 München
Germany
E-Mail: rainer.richter@hll.mpg.de

Preprint No. 630
Berlin 2001

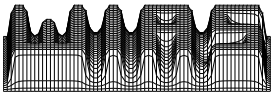

Das diesem Artikel zugrundeliegende Vorhaben wurde mit Mitteln des Bundesministeriums für Bildung und Forschung unter dem Förderkennzeichen 03-GA7FV1-2 gefördert. Die Verantwortung für den Inhalt dieser Veröffentlichung liegt bei den Autoren.

Edited by
Weierstraß–Institut für Angewandte Analysis und Stochastik (WIAS)
Mohrenstraße 39
D — 10117 Berlin
Germany

Fax: + 49 30 2044975
E-Mail (X.400): c=de;a=d400-gw;p=WIAS-BERLIN;s=preprint
E-Mail (Internet): preprint@wias-berlin.de
World Wide Web: http://www.wias-berlin.de/

Abstract

We report on a system of nonlinear partial differential equations describing signal conversion and amplification in semiconductor detectors. We explain the main ideas governing the numerical treatment of this system as they are implemented in our code WIAS–TeSCA. This software package has been used by the MPI Semiconductor Laboratory for numerical simulation of innovative radiation detectors. We present some simulation results focussing on three–dimensional effects in X–ray detectors for satellite missions.

2000 Mathematics Subject Classification

Primary 65M60; Secondary 35K57, 35B40, 65M12.

2001 Physics and Astronomy Classification Scheme (PACS)

Primary 85.60.Gz; Secondary 07.85.Fv, 95.55.Ka.

Key words and phrases

semiconductor device simulation, reaction–diffusion systems, asymptotic behavior, time and 3d–space discretization, software design, X–ray pixel detector, DEPFET, DEPMOS.

Contents

1 Introduction **2**

2 The drift–diffusion model **2**

3 Numerics for the drift–diffusion model **4**

3.1 Calculation of contact currents 4

3.2 Time discretization 4

3.3 Space discretization 5

3.4 Decoupling, Linearization 6

3.5 Solution of linear algebraic equations 6

4 Software Design **7**

5 Simulation results **7**

1 Introduction

For observation of X–ray radiation in astrophysics and other applications semiconductor detectors play a rapidly growing role. Devices as the DEPFET (DEPleted Field Effect Transistor), in particular the MOS–type (DEPMOS) developed at the MPI Semiconductor Laboratory and the Max Planck Institutes for Physics and for Extraterrestrial Physics [9], offer very important advantages when compared to conventional detectors. These advantages are due to the intrinsic feature of the structure which at once has detector and amplifier properties. High amplification and low noise can be obtained and the charge generated by the signal can be read out at the place of origin, therefore avoiding problems connected with charge transport.

For development and optimization of such refined semiconductor detectors mathematical modeling and numerical simulation is indispensable. At the MPI Semiconductor Laboratory the simulation program WIAS–TeSCA is used to design detectors and to anticipate their qualitative and quantitative behavior. Device simulations on a prototype design of DEPFET confirm that the device is intrinsically fast and that it will function properly.

It is the aim of this article to describe the mathematical model for semiconductor detectors and the main ideas underlying our code for numerically solving the model equations reliably and efficiently. Finally we present some simulation results concerning detector structures of current interest.

2 The drift–diffusion model

Charge generation by radiation and charge transport in semiconductor detectors can be described adequately by the drift–diffusion model, consisting of a Poisson equation for the electrostatic potential φ:

$$-\nabla \cdot (\epsilon \nabla \varphi) = d + u_2 - u_1 \qquad \text{in } \Omega \ , \tag{1}$$

and continuity equations for the charge carriers, electrons u_1 and holes u_2:

$$\frac{\partial u_i}{\partial t} - \nabla \cdot (\mu_i \, (\nabla \, u_i \, + \, q_i u_i \nabla \varphi)) = g - r \qquad \text{in } Q \ . \tag{2}$$

Here $\Omega \subset \mathrm{R}^n$, $n \leq 3$, is the Lipschitzian domain, occupied by the detector and $Q = (0,T) \times \Omega$ is a time cylinder. The source term $g = g(t,x)$, $(t,x) \in \Omega$, models charge generation by radiation and the remaining symbols have the following meaning:

$\epsilon = \epsilon(x)$	dielectric permittivity,
$d = d(x)$	density of impurities,
$\mu_i = \mu_i(x, \lvert\nabla \phi_i\rvert)$	mobility,
$\phi_i = \varphi + q_i \log u_i$	electro–chemical potential,
$q_1 = -1, \ q_2 = +1$	sign of charges,
$r = r_0(u)(u_1 u_2 - 1)$	recombination rate,

where the index $i = 1, 2$ refers to electrons and holes respectively, and $u = (u_1, u_2)$ is the vector of charge densities. This system has to be completed by initial conditions

$$u_i(0, x) = u_{i0}(x) \geq 0, \quad x \in \Omega, \quad i = 1, 2 \ , \tag{3}$$

and boundary conditions

$$\begin{aligned} \varphi = \varphi_\Gamma, \quad u_i = u_{i_\Gamma} \qquad & \text{on } (0,T) \times \Gamma_D, \ i = 1, 2, \\ \nu \cdot \nabla\varphi = \nu \cdot \nabla\phi_i = 0 \qquad & \text{on } (0,T) \times \Gamma_N, \ i = 1, 2, \end{aligned} \tag{4}$$

where $\Gamma = \partial\Omega = \Gamma_D \cup \Gamma_N$ and ν is the outer unit normal on Γ.

The drift–diffusion model was derived by van Roosbroeck [13] in 1950 and is now generally accepted. The first significant report on using numerical techniques to solve these equations for carriers in an operating semiconductor device structure has been published by Gummel [7] in 1964. Since then the numerical modeling of semiconductor devices proved to be a powerful tool for device designers.

First mathematical papers devoted to the drift–diffusion equations of carrier transport in semiconductors appeared at the beginning of the seventies [10, 11]. Global existence and uniqueness of solutions under realistic physical and geometrical conditions was proved firstly in [5].

The key for proving these results and also for establishing stable numerical solving procedures is the existence of a Lyapunov function for (1–2), provided

$$u_{i_\Gamma} = \exp(-q_i\varphi_\Gamma), \quad g = 0 \ .$$

Indeed, under these assumptions the free energy

$$\mathcal{F}(\varphi, u) = \int_\Omega \left[\frac{\epsilon}{2} \left| \nabla(\varphi - \varphi^*) \right|^2 + \sum_{i=1}^{2} u_i (\log \frac{u_i}{u_i^*} - 1) \right] dx$$

satisfies

$$\frac{d\mathcal{F}}{dt} = -\int_\Omega \left[\sum_{i=1}^{2} \mu_i u_i |\nabla\phi_i|^2 \ + \ (\phi_2 - \phi_1)\, r \right] dx \leq 0 \ , \tag{5}$$

where the thermal equilibrium potential φ^* is solution of the nonlinear Poisson equation

$$\begin{aligned} -\nabla \cdot (\epsilon \nabla\varphi^*) = d + \exp(-\varphi^*) - \exp(\varphi^*) \qquad & \text{in } \Omega \ , \\ \varphi^* = \varphi_\Gamma \quad \text{on } \Gamma_D, \qquad \nu \cdot \nabla\varphi^* = 0 \quad & \text{on } \Gamma_N \end{aligned}$$

and the equilibrium charge densities are given by

$$u_i^* = \exp(-q_i\varphi^*) \ .$$

In particular, (5) implies exponential decay of the solution (φ, u) to (1–4) to the thermal equilibrium (φ^*, u^*).

3 Numerics for the drift–diffusion model

3.1 Calculation of contact currents

In view of real detector structures we suppose that

$$\Gamma_D = \bigcup_{j=1}^{k_0} K_j \ .$$

An essential task of device simulation in general and of detector simulation in particular, is accurate calculation of the currents J_{K_j} through the device contacts K_j. Since in general, by analytical reasons, only weakly regular solutions can be expected, we calculate the J_{K_j}'s in accordance with the definition of weak solutions. To this end, we provide suitable test functions h_j as solutions of the boundary value problems

$$\Delta h_j = 0 \quad \text{in } \Omega, \qquad \nu \cdot \nabla h_j = 0 \quad \text{on } \Gamma_N, \qquad h_j = \begin{cases} 1 & \text{on } K_j, \\ 0 & \text{on } K_k,\ k \neq j, \end{cases}$$

such that, evidently,

$$\sum_{j=1}^{k_0} h_j \equiv 1 \quad \text{in } \Omega \ . \tag{6}$$

Now, differentiating (1) with respect to time and adding to (2), we get the conservation of total current

$$\nabla \cdot J = 0, \qquad J = \epsilon \nabla \frac{\partial \varphi}{\partial t} + \sum_{i=1}^{2} \mu_i \left(q_i \nabla u_i + u_i \nabla \varphi \right) \ .$$

(J sums up the dielectric displacement current, the electron and hole current.) Hence, the Gauß theorem implies

$$J_{K_j} = \int_{K_j} J \cdot \nu \, ds = \int_{\Omega} J \cdot \nabla h_j \, dx \ ,$$

and as a consequence of (6)

$$\sum_{j=1}^{k_0} J_{K_j} = 0 \ .$$

3.2 Time discretization

For time discretization we apply Euler's implicit method and we regard a partition of the time interval:

$$[0, T] = \cup_j S_j, \quad S_j = [t_{j-1}, t_j], \quad \tau_j := t_j - t_{j-1} > 0, \quad t_0 = 0 \ .$$

Then our time discrete version of the drift–diffusion system reads

$$\begin{aligned} -\nabla\cdot\big(\epsilon\nabla\varphi^j\big) &= d + u_2^j - u_1^j \ , \\ \frac{u_i^j - u_i^{j-1}}{\tau_j} - \nabla\cdot\big(\mu_i^{j-1}\,(\nabla\ u_i^j\ +\ q_i u_i^j\nabla\varphi^j)\big) &= g^j - r^j \ , \\ u_i^0 &= u_{0i} \ , \end{aligned} \tag{7}$$

where $j = 1, 2, \ldots$ indexes the discrete times, and $i = 1, 2$ indicates the species.

An essential feature of this discretization is that, as in the continuous case, the free energy is Lyapunov function. More precisely, there is the following estimate [4]:

$$\frac{\mathcal{F}(\varphi^j, u^j) - \mathcal{F}(\varphi^{j-1}, u^{j-1})}{\tau_j} \le -\int_\Omega \left[\sum_{i=1}^2 \mu_i^{j-1} u_i^j |\nabla\phi_i^j|^2 + (\phi_2^j - \phi_1^j)\, r^j\right] dx \le 0 \ .$$

3.3 Space discretization

For space discretization we use n–dimensional simplex elements E_l such that

$$\Omega = \cup_l E_l \ .$$

By $\mathcal{E}$ we denote the set of all edges $e_{kl} = x_k - x_l$ connecting vertices x_k and x_l of our triangulation. Let

$$V_k = \{x \in \mathrm{R}^n :\ \|x - x_k\| \le \|x - x_j\| \quad \text{for all vertices } x_j \in \Omega\}$$

be the Voronoi cell assigned to vertex x_k and ∂V_k its surface. Our main hypothesis with respect to space discretization is that the electron and hole current $J_i = q_i\mu_i\big(\nabla\ u_i\ +\ q_i u_i\nabla\varphi\big)$, $i = 1, 2$, have to be constant along simplex edges e_{kl}:

$$J_{ikl}(s) = \mu_{ikl} q_i\,(\nabla\ u_i\ +\ q_i u_i\nabla\varphi)\,(s)\ =\ \text{const.}\quad \text{for all } s \in e_{kl} \ .$$

Replacing ∇ by d/ds, we get ordinary differential equations with respect to the edge parameter s. After integration we can express J_{ikl} in terms of the vertex values $\varphi_k = \varphi(x_k)$ and $u_{ik} = u_i(x_k)$:

$$J_{ikl} = \frac{\mu_{ikl} q_i}{|e_{kl}|}\,\big(b\big(q_i(\varphi_k - \varphi_l)\big)u_{il} - b\big(-q_i(\varphi_k - \varphi_l)\big)u_{ik}\big) \ ,$$

where

$$b(s) = \frac{s}{\exp(s) - 1}$$

is the Bernoulli function. In order to derive a space discrete version of the drift–diffusion system, we test (1) and (2) with the characteristic function χ_{V_k} of the Voronoi cell V_k. Thus, applying the Gauß theorem, we arrive at

$$\begin{aligned} \epsilon_k \sum_{\{l:\, e_{kl}\in\mathcal{E}\}} \frac{\varphi_k - \varphi_l}{|e_{kl}|}\big|\partial V_k \cap \partial V_l\big| &= (d_k + u_{2k} - u_{1k})\,|V_k|, \\ \frac{\partial u_{ik}}{\partial t}|V_k| - q_i \sum_{\{l:\, e_{kl}\in\mathcal{E}\}} J_{ikl}\big|\partial V_k \cap \partial V_l\big| &= (g_k - r_k)|V_k| \ , \end{aligned} \tag{8}$$

for all vertices x_k of our triangulation.

As the original drift–diffusion equations (1–2) and its time discrete variant (7), also the space discrete version (8) has the free energy as Lyapunov function. Indeed, there is the following estimate [4]:

$$\frac{d\mathcal{F}}{dt} \le -\sum_{e_{kl}\in\mathcal{E}} \Bigg[\sum_{i=1}^{2} u_{ik}\mu_{ikl} \frac{\left|\partial V_k \cap \partial V_l\right|}{|e_{kl}|} \frac{b(\varphi_l-\varphi_k)}{b(\phi_{il}-\phi_{ik})} \left|\phi_{ik}-\phi_{il}\right|^2 + |V_k|\,(\phi_{2k}-\phi_{1k})r_k \Bigg] \le 0 \quad .$$

Now it is straight forward to combine time and space discretization in such a way that the free energy remains Lyapunov function of the fully discretized drift–diffusion system as it is implemented in our numerical code WIAS–TeSCA.

3.4 Decoupling, Linearization

A natural way of decoupling the drift–diffusion equations is due to Gummel [7]. It starts from the state equations

$$u_i = \exp\left(q_i(\phi_i-\varphi)\right) \quad . \tag{9}$$

Assuming the electro–chemical potentials ϕ_i to be known from a preceding iteration, equation (1) can be seen as a nonlinear elliptic equation with monotone nonlinearity with respect to the electrostatic potential φ and can be solved via a globally convergent Newton procedure. In the second step we insert φ into the continuity equations and solve them for u_i. Finally, from φ and u_i we update the electro–chemical potentials ϕ_i via (9).

Roughly speaking, Gummel's iteration method converges rapidly far away and slowly near the solution. Thus, we could combine it advantageously with Newton's method having a complementary behavior.

3.5 Solution of linear algebraic equations

After space and time discretization, decoupling and linearization we end up with sparse linear equation systems. The Poisson equation is symmetric and can be solved without any problems by conjugate gradient methods. The continuity equations, due to the (in general) strong drift term $\nabla\varphi$, are only structurally symmetric and very stiff. Hence, we are often obliged to go back to direct solution procedures. Fortunately, we have available highly efficient factorization processes with complete super–node pivoting [12].

4 Software Design

Originally WIAS–TeSCA [3] is a two dimensional semiconductor device simulation package written in FORTRAN. The present redesign of WIAS–TeSCA aims at a tool which operates on two and three dimensional spatial domains. WIAS–TeSCA shall deal with a variable set of coupled model equations, which are defined and have to be solved on specific parts of the simulation domain, while referring to and communicating via the underlying discretization of the whole simulation domain. The management of material properties also works within this concept.

In the sense of structured programming we adopt an object oriented approach [6]. The implementation is made in C, while using numerical kernels in FORTRAN. All features which might impede portability, such as special C++ constructions are omitted. We reuse pdelib–components [1], in particular the interface for grid management and the interface for linear algebra. Moreover, we make use of the interactive graphics package gltools [2], and there is an interface to the extension language lua [8] for the description of the simulation problem.

In the following we describe the calculation of the electrostatic potential in a doped semiconductor hetero–structured detector. To that end a nonlinear Poisson equation with prescribed spatially varying quasi Fermi potentials of the carrier densities has to be solved on a fully three dimensional spatial domain.

5 Simulation results

The structure and operation principle of the MOS–type DEPFET is shown in Fig. 1. It is based on the sideward depletion as used in the semiconductor drift chamber and the field effect transistor. The transistor is located atop a low doped n–type semiconductor substrate. It becomes fully depleted by applying a sufficiently high negative voltage to the backside p^+ contact. By suitable doping, a potential minimum for electrons is formed below the transistor channel. The fully depleted bulk is the sensitive volume of the detector in which electron–hole pairs created by the incident radiation are separated by the electric field. While the holes are moved to the negatively biased back–contact, the electrons are collected in the local potential minimum below the channel of the transistor (the so called "internal gate") and thus, increase its charge density by induction. As a consequence, the transistor current is increased as long as the signal charge is not removed from the internal gate. The removal of the signal charge (emptying of the internal gate) can be performed in a way, which will be described below. Arranging many DEPFETs over an extended area leads to a pixel detector array with each single DEPFET providing one pixel.

Our two– and three–dimensional device simulations of pixel cells with WIAS–TeSCA concern the response of the device to radiation (the collection mechanism), the functionality of the emptying of the internal gate (the clearing mechanism), and the transfer of charge between two internal gates. The latter mechanism plays a role in

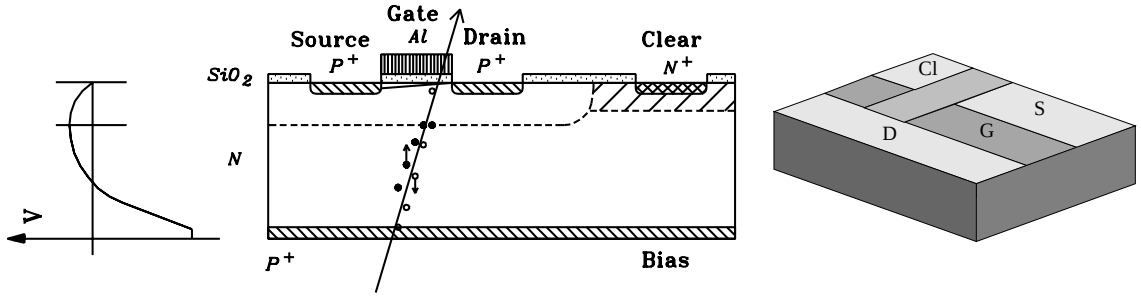

Figure 1: The DEPFET structure

detector arrays, when the option of noise reduction by switching and repeated read out is used, see [9].

A perspective view on the electrostatic potential and the carrier densities in two operating states of a single pixel cell is shown in Figs. 2–5. The pixel cell measures $18\mu\text{m}\times15\mu\text{m}\times280\mu\text{m}$ and the figures show a section of the three dimensional simulation domain up to a depth of 12μm. For this type of topologies care has to be taken to avoid detrimental effects due to the sideward limits of the structure. In the three dimensional plot of the hole density, see Fig. 5, atop the structure the p^+ contacts are visible red shaded. The drain (D) stretches over the full width of the device and is connected with the source (S) through the MOS enhancement channel below the gate (G), see Fig. 1. In the three dimensional plot of the electron density, see Fig. 3, atop the structure the n^+ clear contact (Cl) is visible red shaded. It is separated from the source by the clear gate, see also Fig. 1. The signal charge is stored within the internal gates located below the transistor channel. As the DEPFET transistors are built on detector grade low doped silicon, additional buried n–type doping fairly close to the surface is necessary in order to move the position of the internal gate close to the surface (at a distance smaller than the gate length) and simultaneously prevent the flow of holes from the transistor through the bulk towards the strongly negatively biased backside diode.

Single photon detection of X–rays with a high energy resolution requires the collection of the whole generated signal charge without any losses. Since in the charge collection mode all generated electrons have to drift into the internal gates the still positively biased clear contacts have to be shielded from the sensor region. Fig. 2 shows the build up of a potential barrier beneath the n–doped clear contact by a buried p–doped layer. This layer becomes completely depleted from holes during the clearing phase, where a high positive voltage is applied to the clear contact, see Fig. 5. After turning off the clear voltage the p–doped region remains depleted forming the required potential barrier by the influence of the negative space charge of the acceptor ions. This non steady state can be simulated by applying a locally fixed quasi Fermi potential for holes in the buried p–doped layer.

After each readout the internal gate has to be emptied. Complete clearing of the internal gate avoids noise due to fluctuations in the left–over charge. Clearing of the internal gate is performed by the application of a positive voltage pulse of approx-

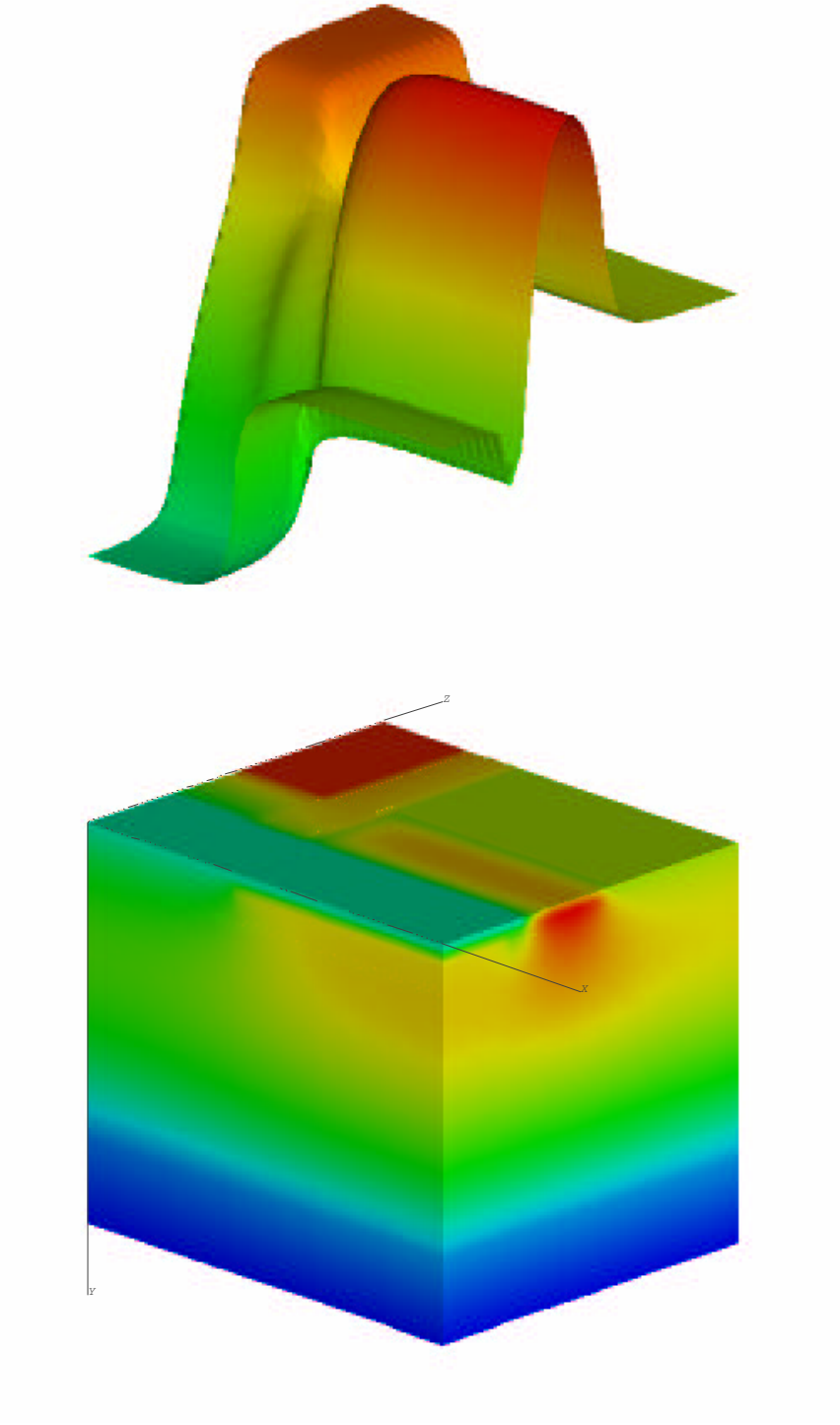

Figure 2: DEPMOS pixel cell in collection mode: electrostatic potential. Bottom: three dimensional plots. Top: level plots at a depth of 500nm.

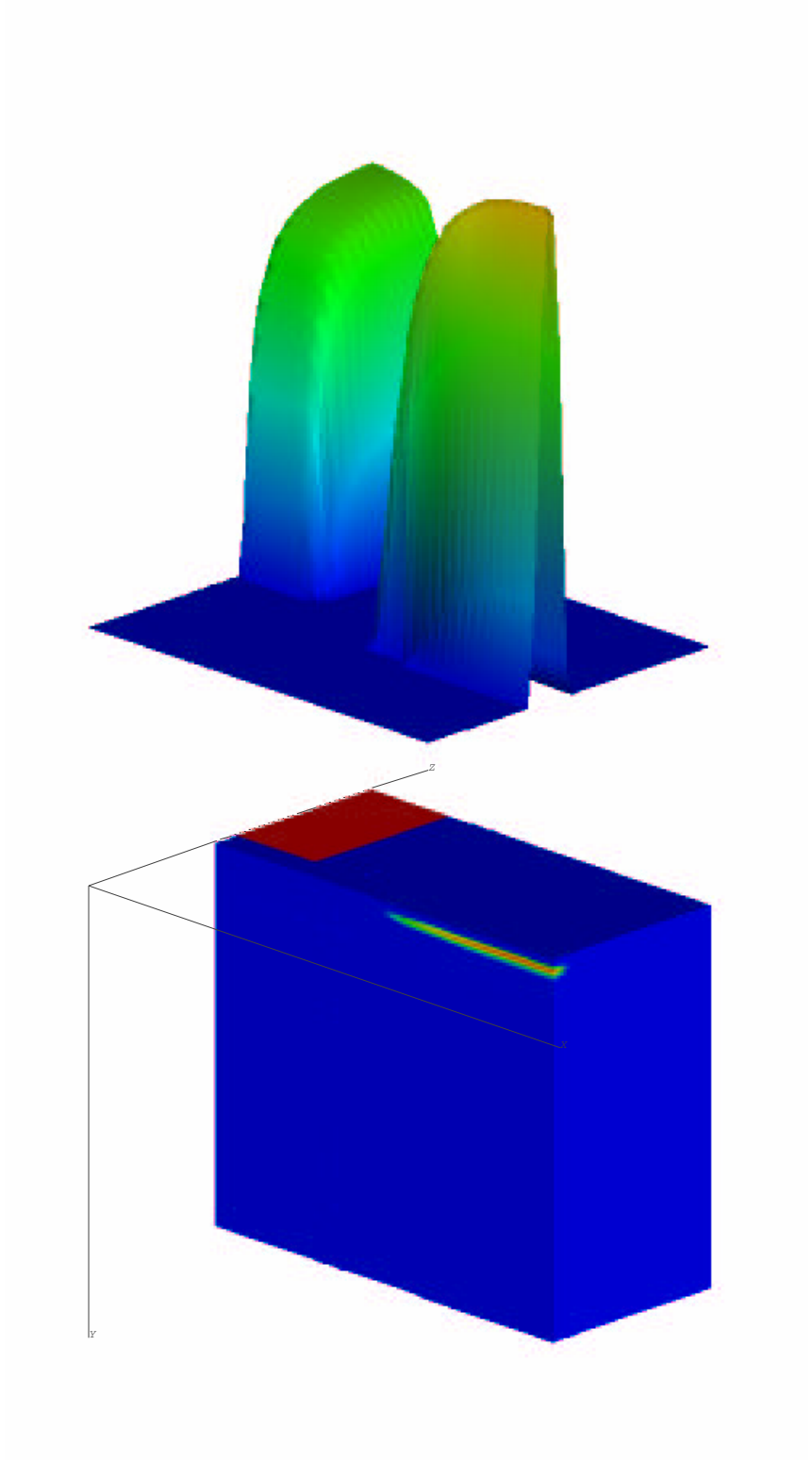

Figure 3: DEPMOS pixel cell in collection mode: electron density. Bottom: three dimensional plots. Top: level plots at a depth of 500nm.

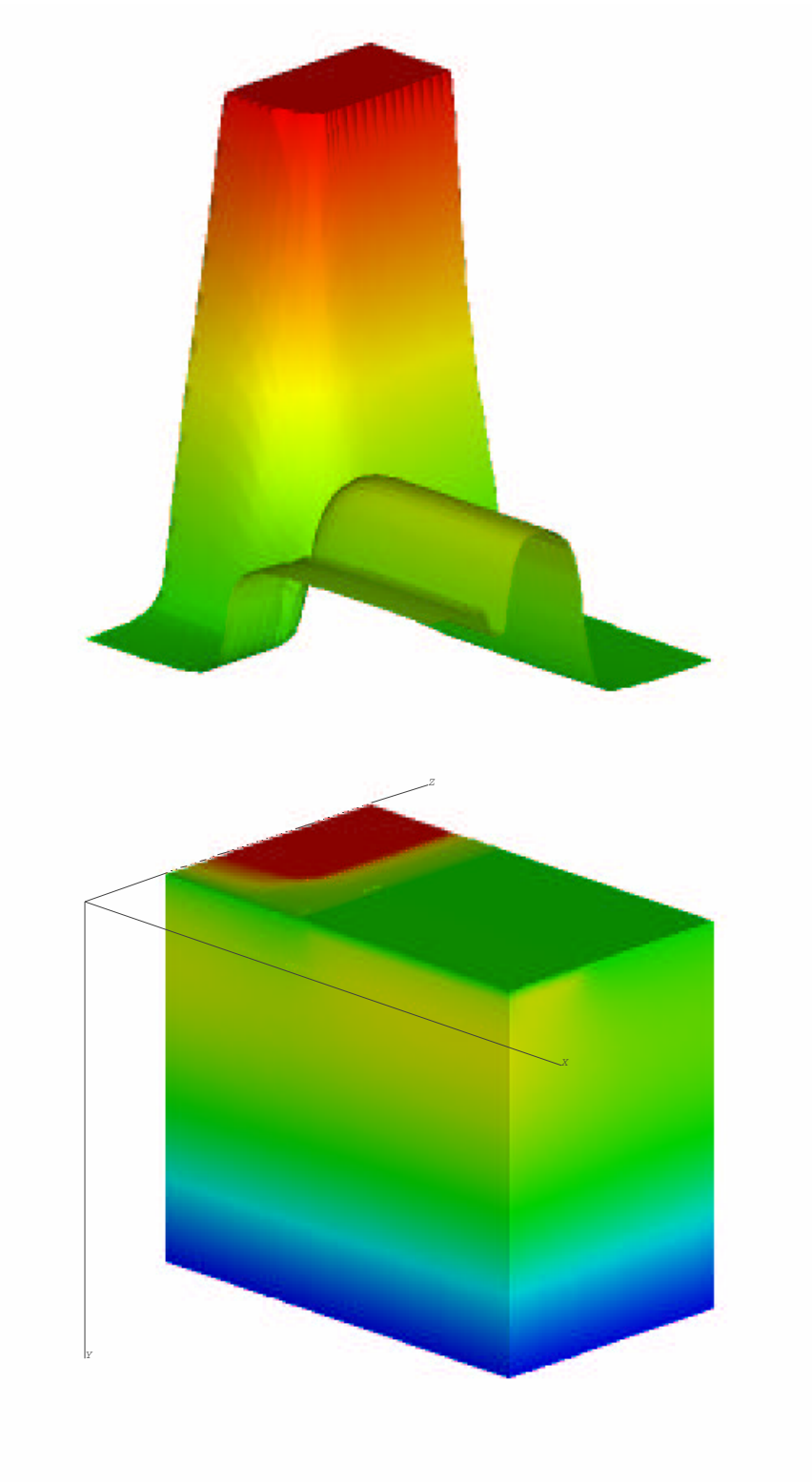

Figure 4: DEPMOS pixel cell in clearing mode: electrostatic potential. Bottom: three dimensional plots. Top: level plots at a depth of 200nm.

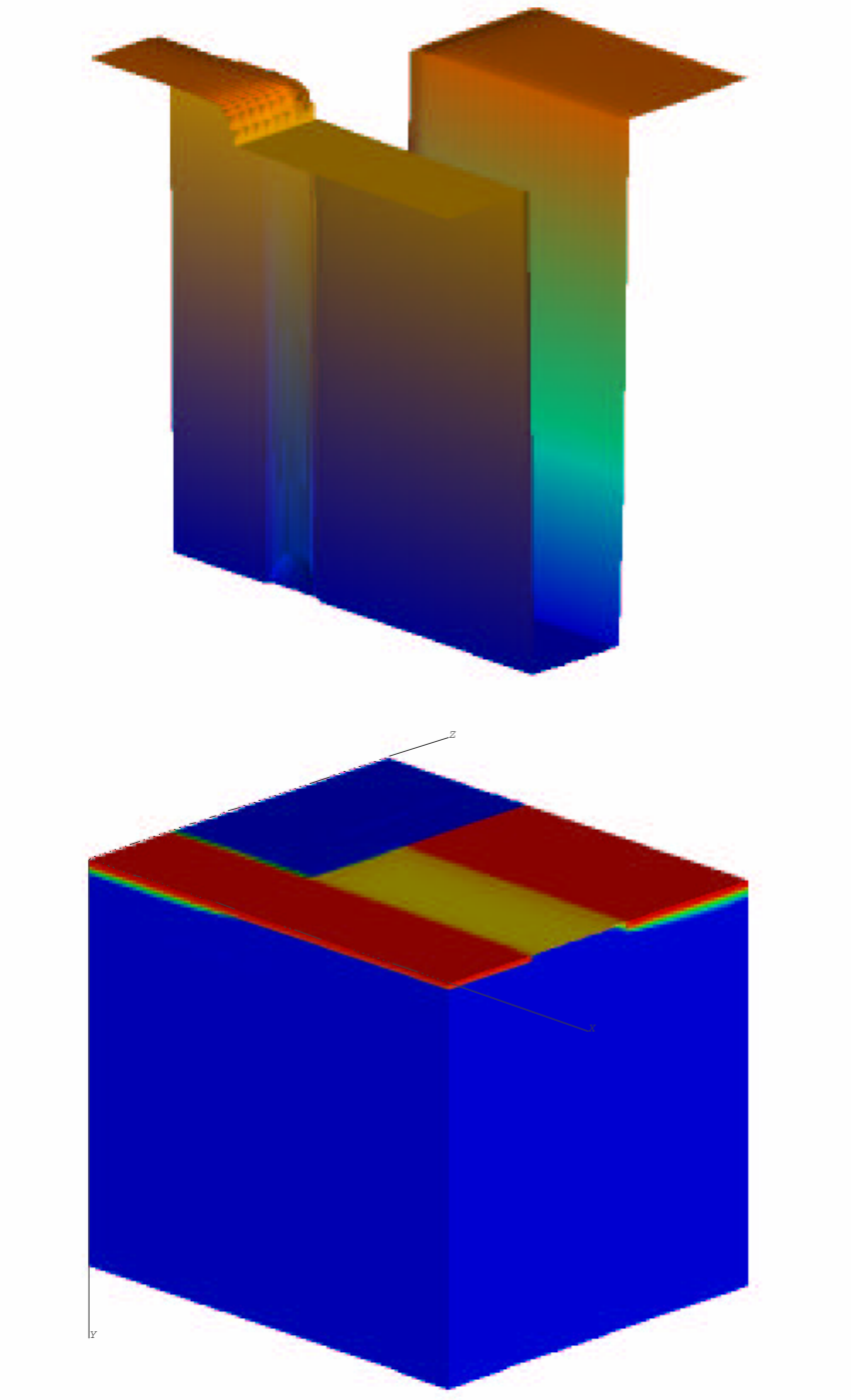

Figure 5: DEPMOS pixel cell in clearing mode: hole density.
Bottom: three dimensional plots. Top: level plots at a depth of 200nm.

imately 12V to the clear contact. Fig. 4 displays a potential barrier between the internal gate and the n^+ clear contact. Such a barrier hinders the clearing mechanism and its removal was a task for further optimization of the device. Proper adjustment of device layout, doping profiles and applied voltages leads to detector structures which are intrinsically very fast such that the read out and clearing speed will rather be limited by effects in the signal routing.

Acknowledgments

We thank Gerd Reinhardt (WIAS Berlin) for his support with the graphics.

References

[1] J. Fuhrmann, Th. Koprucki, and H. Langmach, *pdelib: An open modular tool box for the numerical solution of partial differential equations. design patterns.*, Proceedings of the 14th GAMM Seminar on Concepts of Numerical Software (W. Hackbusch and G. Wittum, eds.), Notes on Numerical Fluid Mechanics, Vieweg Verlag, 1998, submitted.

[2] J. Fuhrmann and H. Langmach, *gltools*, Weierstrass Institute for Applied Analysis and Stochastics, Mohrenstraße 39, D–10117 Berlin, http://www.wias-berlin.de/~gltools.

[3] H. Gajewski et al., TeSCA *Two– and three–dimensional SemiConductor Analysis package*, Weierstrass Institute for Applied Analysis and Stochastics, Mohrenstraße 39, 10117 Berlin, Germany.

[4] H. Gajewski and K. Gärtner, *On the discretization of van Roosbroeck's equations with magnetic field*, Technical Report 94/14, Eidgenössische Technische Hochschule Zürich, Institut für Integrierte Systeme, 1994.

[5] H. Gajewski and K. Gröger, *On the basic equations for carrier transport in semiconductors*, Jnl. of Math. Anal. Appl. **113** (1986), 12–35.

[6] E. Gamma, R. Helm, R. Johnson, and J. Vlissides, *Design patterns, elements of reusable object–oriented software*, Addison–Wesley, Reading, Mass., 1995.

[7] H. K. Gummel, *A self–consistent iterative scheme for one–dimensional steady state calculations*, IEEE Transactions on Electron Devices **11** (1964), 455.

[8] R. Ierusalimschy, L. H. de Figueiredo, and W. Celes, *Lua - an extensible extension language*, Software: Practice & Experience **26** (1996), no. 6, 635–652.

[9] G. Lutz, R. H. Richter, and L. Strüder, *DEPMOS–Arrays for X–ray imaging*, XRAY Optics, Instruments and Missions III (J. Trümper and B. Aschenbach, eds.), Proceedings of SPIE, vol. 4012, 2000, pp. 249–256.

[10] M. S. Mock, *On equations describing steady–state carrier distributions in a semiconductor device*, Comm. Pure Appl. Math. **25** (1972), 781–792.

[11] ———, *An initial value problem from semiconductor device theory*, SIAM J. Math. Anal. **5** (1974), 597–612.

[12] O. Schenk, *Scalable parallel sparse LU factorization methods on shared memory multiprocessors*, Series in Microelectronics, vol. 89, Hartung–Gorre Verlag, Konstanz, 2000.

[13] W. van Roosbroeck, *Theory of the flow of electrons and holes in Germanium and other semiconductors*, Bell System Technical Journal **29** (1950), 560.